Resolving the Connectivity-Throughput Trade-Off in Random Networks

Ralph Tanbourgi, Holger Jäkel, Friedrich K. Jondral

Abstract

The discrepancy between the upper bound on throughput in wireless networks and the throughput scaling in random networks which is also known as the connectivity-throughput trade-off is analyzed. In a random network with λ nodes per unit area, throughput is found to scale by a factor of $\sqrt{\log \lambda}$ worse compared to the upper bound which is due to the uncertainty in the nodes' location. In the present model, nodes are assumed to know their geographical location and to employ power control, which we understand as an additional degree of freedom to improve network performance. The expected throughput-progress and the expected packet delay normalized to the one-hop progress are chosen as performance metrics. These metrics are investigated for a nearest neighbor forwarding strategy, which benefits from power control by reducing transmission power and, hence spatial contention. It is shown that the connectivity-throughput trade-off can be resolved if nodes employ a nearest neighbor forwarding strategy, achieving the upper bound on throughput on average also in a random network while ensuring asymptotic connectivity. In this case, the optimal throughput-delay scaling trade-off is also achieved.

I. Introduction

Wireless (multi-hop) networks have recently gained much regard due to steady advances in the development of inexpensive communication devices as well as due to the growing interest in infrastructureless applications, e.g., ad hoc or sensor networks. It is fundamental to these networks that communication does not rely on a wired backbone, resulting in that nodes must additionally undertake the task of forwarding other nodes' packets. This, of course, gives rise to some new questions in network design among several layers. Issues are, e.g., resource allocation, energy expenditure and security aspects. On the medium access control (MAC) layer the probably most interesting question is how to achieve an appropriate balance between increasing a node's performance on the one hand and increasing the overall network performance on the other hand. This question is difficult to answer since nodes are expected to share a common transmission bandwidth, resulting in the fact that network performance is limited by self-interference: increasing a node's transmission power improves link quality but at the same time increases interference to other nodes.

The authors are with the Communications Engineering Lab (CEL) at the Karlsruhe Institute of Technology (KIT), Germany. Email: {ralph.tanbourgi, holger.jaekel, friedrich.jondral}@kit.edu. The contact author is R. Tanbourgi. This manuscript was submitted to the IEEE Transaction on Information Theory on July 15, 2010.

A lot of effort has been made to analyze the capacity of (self-interference limited) wireless networks within the last decade. In [1], the authors proved that there exists an upper bound on throughput which scales as[1] $\Theta\left(\frac{1}{\sqrt{\lambda}}\right)$, where λ denotes the number of nodes per unit area, i.e., the node density. In [1] the authors also presented a constructive proof for the existence of a global scheduling scheme for which throughput is $\Theta\left(\frac{1}{\sqrt{\lambda \log \lambda}}\right)$ in a random network. The proof is based on Voronoi-tessellations, on the assumption of fixed transmission powers, and on routing over straight lines. The same result was obtained using a different strategy in [2]. The gap between this result and the upper bound is due to the additional uncertainty within random networks related to connectivity: for a random network to be asymptotically connected, the transmission range must be proportional to $\sqrt{\frac{\log \lambda}{\lambda}}$ according to [3], resulting in that the average number of neighboring nodes and hence spatial contention increases with $\log \lambda$. Thus, spatial reuse decreases by a factor of $\frac{1}{\log \lambda}$ which explains the discrepancy between the throughput result for random networks and the upper bound.

In [4] the authors showed that the upper bound on throughput is feasible also in random networks if the requirements on connectivity can be relaxed. They use percolation theory arguments and consider the network in the supercritical regime rather than to ensure global connectivity among the nodes. The supercritical regime arises when the transmission range of the nodes is chosen to be just above the percolation threshold. For successful percolation, the transmission range must be $\frac{c}{\sqrt{\lambda}}$, where c is the percolation threshold. In this transition region, a number of paths crossing the network emerge. Packets are then routed along these paths or highways, representing the wireless backbone of the network. On these paths, spatial contention remains constant with increasing λ. However, as the source as well as the destination node might not be directly connected to a highway, this strategy involves a complicated routing scheme consisting of four phases.

Comparing the two works [1] and [4], one can observe a throughput-connectivity trade-off in random networks: if connectivity is assured, the network is driven in an interference limited regime and throughput is $\sqrt{\log \lambda}$ times lower than the upper bound. On the other hand, the upper bound on throughput is achievable if requirements on connectivity are relaxed, resulting into a more complex routing scheme.

Fundamental to both models is that a fixed transmission power is assumed. This gives rise to the following question: if we deflect from the assumption of fixed transmission powers, is it possible to ensure connectivity in a random network (for the purpose of a simple routing scheme) and to afford low spatial contention (to achieve the upper bound on throughput) at the same time?

This work represents an extension in the sense that nodes are allowed to employ power control. In fact, we understand power control as an additional degree of freedom that may resolve the connectivity-throughput trade-off and improve network performance. In our network model, the transmission range is chosen to ensure global connectivity of the network as done in [1]. However, nodes may reduce their transmission power by transmitting to specific nodes within their range, e.g., to their nearest neighbor. To the best of the authors' knowledge, investigation of throughput and delay scaling behavior for random networks where nodes employ power control has not been

[1]In the Landau notation: the term $f(x) = \Theta\left(g(x)\right)$ denotes the fact that $c_0|g(x)| \leq |f(x)| \leq c_1|g(x)|$ for $c_0, c_1 < +\infty$ and $x \to +\infty$.

investigated yet. Taking into account each node's transmission power would of course increase the complexity of the analysis significantly. It is also for this reason why we deflect from prior approaches, where results on throughput were proven to apply with high probability as λ tends to infinity. In contrast, our approach aims at investigating the average per-node throughput and average delay as λ increases. We therefore analyze the *expected* throughput and the *expected* delay for a given set of parameters, e.g., channel model, interference model, traffic pattern etc. These two measures are consistent with prior results in the scaling sense.

The results presented in this work are based on the protocol model according to [5] and apply to wireless networks with random traffic patterns. Furthermore, the impact of fading on network performance is not considered here and path loss is assumed to be perfectly compensated by power control. The MAC is modeled as a reservation-based time division multiple access (TDMA) scheme. In contrast to other strategies such as Aloha or carrier sense multiple access (CSMA), a reservation-based MAC is optimal[2] in terms of throughput. Furthermore, greedy geographic forwarding (GGF) is used to model the nearest neighbor forwarding strategy. GGF is chosen because it seamlessly fits to the statistical network model and because it is memoryless and thus allows the analysis of only one hop to be representative. Furthermore, GGF has a high practical relevance for (mobile) ad hoc networks due to its scalability. In the GGF framework, the nearest neighbor forwarding approach is represented by the "nearest with forward progress" (NFP) strategy [6]. This strategy reduces interference in the network to a minimum extend by transmitting only to the nearest neighbor node that gives positive progress to the routing process. A complementary strategy would be for example the "most forward with variable radius" (MVR) strategy [6], which intends to maximize the one-hop progress toward the destination node and thus maximizes interference or spatial contention associated with one hop. This approach is found to be a good approximation for shortest path routing in dense networks [7]. We expect that per-node throughput will increase if NFP is used, since this strategy aims at maximizing spatial reuse. The increase in throughput will consequently lead to a higher delay, since packets are delivered over more hops [18].

A. Related Work

Capacity and throughput scaling laws have been intensively studied in the literature, see for example [1], [2], [4], [5], [8]. Furthermore, [9] analyzed the scaling behavior of a realistic 802.11 MAC. A different approach for analyzing performance in wireless networks is done in [10], [11]. Here, transmission capacity rather than end-to-end rate or transport capacity is investigated. Transmission capacity is defined as the number of successful transmissions taking place simultaneously subject to a constraint on outage probability. This quantity is consistent with end-to-end rate and transport capacity in the scaling sense. In [11], a summary of recent results in this framework is given and a so-called uncertainty cube is presented. This cube illustrates the three axes of uncertainty, namely the node location, the channel fading and the channel access.

The throughput-connectivity trade-off was highlighted in [12], [13]. In [12], the impact of different attenuation functions on connectivity and capacity was investigated where it was found that there exist a fundamental trade-off

[2]We neglect the complexity as well as the signaling overhead of the contention procedure.

between throughput and connectivity. In [13], the authors proved that the per-node throughput remains constant with increasing λ, if an arbitrary small fraction of nodes is allowed to be disconnected from the network.

B. Contribution

Denote by

$$\mathcal{T} := \mathbb{E}\Big\{ C\, Z \Big\} \text{ bit m/s} \tag{1}$$

the expectation of the product of throughput and progress associated with one hop, where C is the per-node throughput or effective (point-to-point) rate in terms of bit per seconds and Z is the one-hop progress toward the destination in meters. Hence, $\mathcal{T}$ measures how much information has been carried how many meters toward the destination in one second in one hop for one node on average.

Denote by

$$\mathcal{D} := \mathbb{E}\Big\{ \alpha\, Z^{-1} \Big\} \text{ s/m} \tag{2}$$

the average packet delay α normalized to the one-hop progress in seconds per meter. Following the definition in [18], packets are scaled by the throughput to keep service time constant in order to capture the delay caused by the network dynamics. Thereby, α accounts for the constant one-hop delay, resulting from, e.g., signal processing at the relay. Then, we have the following results:

Theorem 1: If all nodes employ a nearest neighbor forwarding strategy, we obtain

$$\mathcal{T} = \Theta\left(\frac{1}{\sqrt{\lambda}}\right)$$

and

$$\mathcal{D} = \Theta\left(\sqrt{\lambda}\right).$$

The remainder of the paper is organized as follows. First, the network model is presented in Section II and the statistical modeling of the spatial contention is explained in Section III. We then give an outline of the solution in Section IV and discuss the implications of these results in Section V. Section VI concludes the paper.

II. Network Model

A. Network geometry

A collection of homogeneous nodes $\{X_i\}$ is assumed to be uniformly and independently distributed on a sphere A with unit area according to a stationary Poisson point process (PPP) with intensity λ. Let X_i denote the i-th node as well as its location on A. The PPP is conditioned on having λ nodes on A. Note that this does not affect the distribution of the PPP [14]. The advantage of choosing the sphere rather than some other geometrical topology is that it exhibits a finite surface and avoids unpleasant border effects. Furthermore, it allows local observations to be two-dimensional. Initially, each node independently decides whether to originate a packet or to remain silent with probability equal to the network load p, where $0 < p \leq 1$. We further assume that a node can be a destination node only for one source node in order to ensure that traffic is homogeneous on A. In addition, a source node does not

generate a new packet until the previous packet has reached the destination node. All nodes have omnidirectional antennae and obey a maximum transmission power constraint. Furthermore, they are allowed to temporally store an arbitrary number of packets before forwarding. The network is considered at a snapshot of time.

B. Communications model

As a result of the constraint on maximum transmission power, a node is allowed to communicate directly only with nodes located within its proximity. Here, the motivation for this constraint is that it limits the amount of spatial contention in the network. However, if the range of transmissions is not sufficiently large, global connectivity of the network can not be assumed. We therefore set the transmission range equal to the critical radius r_c, i.e., the required radius for which global connectivity is ensured with probability $1-\epsilon$, where $0<\epsilon\ll 1$. The critical radius r_c is derived in Appendix VII. Nodes are further assumed to adjust their transmission power such that the path loss is compensated and a certain signal-to-noise ratio (SNR) is achieved at the receiver. Thus, the maximum transmission power is the power that achieves the target SNR for a node at distance r_c.

All nodes share a common transmission bandwidth, which is not divided into sub bands. Without loss of generality, we assume that this bandwidth is equal to one Hz resulting in that all nodes transmit at rate η bits per seconds, where η is the spectral efficiency. We further assume that all packets have the same length.

C. Interference model

We use the protocol model to characterize interference. The protocol model states that for *successful* transmission from a transmitter X_i to a receiver X_j it is required that

$$|X_k - X_j| \geq (1+\Delta)\,|X_k - X_\ell| \tag{3}$$

holds for all other transmitter-receiver pairs X_k and X_ℓ [5]. The parameter Δ specifies a guard zone around the receiver which is an increasing function of the spectral efficiency η: if transmissions are with high spectral efficiency η the required signal-to-interference-plus-noise ratio (SINR) will be high, too. Consequently, interfering neighbors must be farther away so that their emitted power can decay fast enough.

While (3) characterizes interference from the viewpoint of the receiver X_j, we propose a second inequality that considers interference from the viewpoint of the transmitter: for an *interference-free* transmission from transmitter X_i to receiver X_j it is required that

$$|X_i - X_\ell| \geq (1+\Delta)\,|X_i - X_j| \tag{4}$$

holds for all other receivers X_ℓ.

D. MAC scheme

We assume that transmissions are locally coordinated by the nodes themselves such that each node obtains a time slot in which it can access the medium. This corresponds to a reservation-based TDMA scheduling scheme.

Building on the protocol model, a transmission does not experience interference if it is scheduled properly. By properly scheduled we mean that both (3) and (4) hold. Hence, the performance bottleneck is not the interference at the receiver but the split of transmissions in time domain resulting from the spatial contention. We will therefore approximate the effective rate C by the inverse of the number of transmissions that violate either (3) or (4).

E. Routing scheme

We assume that nodes use GGF as routing scheme. In GGF, a node currently holding a packet selects one of its neighbors as relay such that an Euclidean metric is optimized. A node must therefore know its own as well as its neighbors' location and, given it is a source node, it must also know the (approximate) location of the destination node. Generally, GGF may fail due to void areas or node mobility. We will not treat this problem here and assume that GGF does not fail at all. We will also not address the problem of providing location information to nodes. See [15] for details.

We define by R_{ij} the transmission radius, i.e., the distance between transmitting node X_i and its corresponding receiver X_j, as

$$R_{ij} := |X_i - X_j| \,. \tag{5}$$

Furthermore, we define by Z_{ij} the progress, which is the distance between a transmitting node X_i and its corresponding receiver X_j projected onto a line connecting X_i and its corresponding destination node X_d, i.e.,

$$Z_{ij} := \frac{\left(\vec{X}_j - \vec{X}_i\right)^T \left(\vec{X}_d - \vec{X}_i\right)}{\left|\vec{X}_d - \vec{X}_i\right|}. \tag{6}$$

The NFP strategy was first introduced in [6] and extended by [16] toward a more general forwarding area. In this strategy, node X_i selects node X_{j^*} as relay if it is in the forwarding area and the transmission radius R_{ij} is minimized, i.e.,

$$\begin{aligned} j^* = \arg\min_j \{R_{ij}\} \\ \text{s.t. } Z_{ij} > 0, \\ R_{ij} \le r_c, \\ \measuredangle\left(\vec{X}_j - \vec{X}_i, \vec{X}_d - \vec{X}_i\right) \le \frac{\gamma}{2}, \end{aligned} \tag{7}$$

where the three constraints describe the forwarding area (see Fig. 1). If nodes are distributed according to a homogeneous PPP, the probability density function (PDF) of the distance R is given by the Rayleigh distribution [16]

$$f_R(r) = \lambda\gamma r\, e^{-\lambda\frac{\gamma}{2}r^2}, \quad r \ge 0. \tag{8}$$

We condition (8) on the fact that the nearest neighbor is always within distance r_c and neglect the normalization term $\frac{1}{1-e^{-\lambda\gamma r_c^2}}$, i.e.,

$$f_{R|r_c}(r) = \frac{f_R(r)}{1 - e^{-\lambda\gamma r_c^2}} \simeq f_R(r), \quad 0 \le r \le r_c. \tag{9}$$

With $1-\epsilon$ denoting the probability of global connectivity, it can be shown that the resulting approximation error is less than $\frac{\epsilon/\lambda}{1-\epsilon/\lambda}$ and hence, $\lim_{(\epsilon/\lambda)\to 0} f_{R|r_c}(r|r_c) = f_R(r)$.

We will also use the PDF of Z conditioned on R. We can obtain this by simple transformation of random variables, yielding

$$f_{Z|R}(z|r) = \frac{2}{\gamma\sqrt{r^2-z^2}}, \quad r\cos(\gamma/2) \le z \le r. \tag{10}$$

III. Statistical Modeling of Medium Access

As mentioned before, the effective rate C for a typical transmitter-receiver pair is anti-proportional to the number of violations of (3) and (4). Recall that the two equations consider interference from the viewpoint of the receiver and the transmitter, respectively. We will model both cases separately.

A. Modeling from the Receiver's Viewpoint

Let the random variable I_{Rx} denote the number of violations of (3) for a typical receiver node X_j, which is called the reference receiver in the following. Since the PPP is stationary, we can assume without loss of generality that the reference receiver is located in the origin. According to Slivnyak's Theorem, the distribution of a PPP conditioned on having a point is identical to the distribution of the original PPP [14]. Thus, I_{Rx} can be written as an independently marked PPP

$$I_{\text{Rx}} = \sum_k K_k M_k, \tag{11}$$

where K_k is a Bernoulli random variable with success probability p and the marks $M_k \in \{0,1\}$ indicate that node X_k is sufficiently close to create an outage at the reference receiver. The marks K_k realize a thinning of the original PPP with thinning factor equal to the network load p (we count only the transmitters). The conditional PDF of the marks M_k given position x_k follows directly from (3)

$$f_{M_k|X_k}(m_k|x_k) = \begin{cases} \mathbb{P}\Big\{(1+\Delta)R_{k\ell} \ge |x_k|\Big\}, & m=1 \\ \mathbb{P}\Big\{(1+\Delta)R_{k\ell} < |x_k|\Big\}, & m=0, \end{cases} \tag{12}$$

where the $R_{k\ell}$ is the distance between a transmitter X_k and its corresponding receiver X_ℓ. Note that the M_k are i.i.d., since every node independently chooses its transmission radius according to the same distribution. The indices k and ℓ in (12) can therefore be omitted. The intensity Λ_{Rx} of the Poisson random variable I_{Rx} is calculated as

$$\begin{aligned} \Lambda_{\text{Rx}} &= p\lambda \int_A \mathbb{P}\left\{(1+\Delta)R \ge |x|\right\} \,\mathrm{d}x \\ &= p\lambda \int_A \left[1 - F_{R|r_c}\left(|x|(1+\Delta)^{-1}\right)\right] \,\mathrm{d}x, \end{aligned} \tag{13}$$

where $F_{R|r_c}(r) = \mathbb{P}\{R \le r | r_c\}$ is the cumulative density function (CDF) of R conditional on the fact that the nearest neighbor is within r_c. Note that $1 - F_{R|r_c}\left(|x|(1+\Delta)^{-1}\right) = 0$ for $|x| > (1+\Delta)r_c$, since transmitters situated outside

a disc $d\left(0;(1+\Delta)r_c\right)$ centered around the receiver (located in the origin) cannot interfere at the receiver due to the fact that the transmission range is limited to r_c. Thus, (13) can be rewritten as

$$\Lambda_{\text{Rx}} = p\lambda \int_{d(0;(1+\Delta)r_c)} \left[1 - F_{R|r_c}\left(|x|\,(1+\Delta)^{-1}\right)\right] \mathrm{d}x.$$

Transforming this into polar coordinates and applying the substitution $\tilde{r} = \frac{r}{1+\Delta}$ yields

$$\Lambda_{\text{Rx}} = 2p\pi\lambda(1+\Delta)^2 \int_0^{r_c} \tilde{r}\left[1 - F_{R|r_c}(\tilde{r})\right] \mathrm{d}\tilde{r}. \tag{14}$$

The conditional CDF $F_{R|r_c}(r)$ is obtained from (9) giving

$$F_{R|r_c}(r) \simeq 1 - e^{-\lambda\frac{\gamma}{2}r^2}, \quad 0 \le r \le r_c. \tag{15}$$

With (14) and (15) we obtain the intensity of I_{Rx} for the case when all nodes employ NFP forwarding, according to

$$\begin{aligned}
\Lambda_{\text{Rx}} &= 2p\pi\lambda\,(1+\Delta)^2 \int_0^{r_c} \tilde{r} e^{-\lambda\frac{\gamma}{2}\tilde{r}^2}\,\mathrm{d}\tilde{r} \\
&= 2p\frac{\pi}{\gamma}\,(1+\Delta)^2\left(1 - \tfrac{\epsilon}{\lambda}\right) \\
&\simeq 2p\frac{\pi}{\gamma}\,(1+\Delta)^2, \qquad (16)
\end{aligned}$$

where the last line follows from the fact that $\frac{\epsilon}{\lambda} \ll 1$. Denoting by $\beta := p\,(1+\Delta)^2$ the traffic intensity, which is the product of the network load and a function of the spectral efficiency, we can rewrite (16) as

$$\Lambda_{\text{Rx}} = 2\beta\frac{\pi}{\gamma}. \tag{17}$$

B. Modeling from the Transmitter's Viewpoint

We denote by the random variable I_{Tx} the number of violations of (4) for a typical transmitter node X_i, which is called the reference transmitter in the following. Here, we assume that the reference transmitter is located in the origin. The number of violations I_{Tx} can be modeled as a weighted PPP, according to

$$I_{\text{Tx}} = \sum_{\ell} K_\ell\,\mathbb{P}\left\{R_{ij}(1+\Delta) \ge |X_\ell|\right\}, \tag{18}$$

where $\mathbb{P}\left\{R_{ij}(1+\Delta) \ge |X_\ell|\right\}$ is a function of both the transmission radius R_{ij} between the reference transmitter X_i and its corresponding receiver X_j and of the distance from reference transmitter X_i to a receiving node X_ℓ. The marks K_ℓ are Bernoulli random variables that realize the thinning of the PPP with thinning factor equal to network load p (we count only the receivers). The term $\mathbb{P}\left\{R_{ij}(1+\Delta) \ge |X_\ell|\right\}$ in (18) can be seen as a weighting of the PPP. The intensity $\Lambda_{\text{Tx}|R}$ of the Poisson random variable I_{Tx} conditioned on the fact that the transmission radius is $R_{ij} = r$ is calculated as

$$\Lambda_{\text{Tx}|R}(r) = p\lambda \int_A \mathbb{1}\left(|x| \le r(1+\Delta)\right) \mathrm{d}x. \tag{19}$$

Since the transmission range R is limited to r_c, a receiver situated outside a disc $d\left(0;(1+\Delta)\,r_c\right)$ centered around the transmitter (located in the origin) cannot be in outage by this transmitter. Hence, the integration range A can be replaced by $d\left(0;(1+\Delta)\,r_c\right)$.

$$\begin{aligned}\Lambda_{\text{Tx}|R}(r) &= p\lambda \int_{d(0;(1+\Delta)r_c)} \mathbb{1}\left(|x| \leq r(1+\Delta)\right)\,\mathrm{d}x \\ &= p\lambda \int_{d(0;(1+\Delta)r)} \mathrm{d}x \\ &= p\lambda\pi\left(1+\Delta\right)^2 r^2 = \lambda\pi\beta r^2. \end{aligned} \tag{20}$$

C. Optimistic and Pessimistic Modeling

The number of violations I associated with a transmission is certainly made up of the violations I_{Rx} experienced by the receiver as well as the violations I_{Tx} caused by the transmitter. However, we can not simply take the sum of I_{Rx} and I_{Tx} since this would overrate the true I for the following reason: consider the two transmitter-receiver pairs $\{X_i, X_j\}$ and $\{X_k, X_\ell\}$. If the transmitter X_k is sufficiently close to the receiver X_j and the transmitter X_i is sufficiently close to the receiver X_ℓ then both (3) and (4) are violated. Consequently, one would count two violations although each transmitter-receiver pair experiences only one violation. Fig. 2 illustrates this problem.

To cope with this problem, we suggest an optimistic as well as a pessimistic modeling of I in order to bound the number of violations I. In the optimistic case, I is given by I_{Tx} only. This corresponds to assuming that all violations from the viewpoint of the receiver are already captured by I_{Tx} which can be seen as a lower bound on I. In contrast, a pessimistic modeling for I is given by assuming independence between I_{Rx} and I_{Tx} and considering their superposition, which is Poisson with intensity $\Lambda_{\text{Rx}} + \Lambda_{\text{Tx}}$. This can be seen as an upper bound on I.

IV. The Solution

Due to the stationarity of the PPP it is sufficient to consider only one typical transmission, which we will call the *reference* transmission in the following. The reference transmission represents the point-to-point link between the reference transmitter and the corresponding reference receiver. Note that the reference transmitter is not necessarily a source node, but may be a relay as we consider the network in a randomly chosen snapshot. The rate (normalized to 1 Hz) at which the packet is transmitted is η. However, if we account for the split in time due to the TDMA MAC, we have to consider the effective rate C, which is generally less than η. The effective rate C depends on the environment seen by both the reference transmitter and the reference receiver through the protocol model or more precisely, C depends on the number of violations I associated with the reference transmission. Hence, for successful transmission, TDMA scheduling implies that

$$C = \frac{\eta}{I+1} \text{ bit/s/Hz}. \tag{21}$$

Note that C is a random variable which depends on I, where I depends on the transmission radius R. To compute $\mathcal{T}$, (21) is further multiplied by the one-hop progress Z. The resulting expression is then averaged with respect to

the uncertainties C, Z and R. Note that C and Z are dependent, since Z and R are. In the following, we will set the spectral efficiency $\eta = 1$ and the constant one-hop delay $\alpha = 1$. This will however not affect the scaling results.

A. Expected Throughput-Progress

To calculate $\mathcal{T}$ we decompose (1) according to the law of total expectation, yielding

$$\mathcal{T} = \mathbb{E}\left\{\mathbb{E}\left\{Z|R\right\}\mathbb{E}\left\{C|R\right\}\right\}. \tag{22}$$

Note that $\mathbb{E}\left\{Z|R\right\}$ and $\mathbb{E}\left\{C|R\right\}$ are independent. With (10), $\mathbb{E}\left\{Z|R\right\}$ is calculated as

$$\mathbb{E}\left\{Z|R\right\} = \frac{2R\sin(\gamma/2)}{\gamma}. \tag{23}$$

In case of $\mathbb{E}\left\{C|R\right\}$, we obtain two expressions, i.e., $\mathbb{E}^{\text{op}}\left\{C|R\right\}$ and $\mathbb{E}^{\text{pe}}\left\{C|R\right\}$, according to the optimistic and the pessimistic modeling of I. The expected optimistic rate $\mathbb{E}^{\text{op}}\left\{C|R\right\}$ conditional on R is written as

$$\begin{aligned}\mathbb{E}^{\text{op}}\left\{C|R\right\} &= \mathbb{E}\left\{\frac{1}{I_{\text{Tx}}+1}\middle|R\right\}\\ &= \sum_{k=0}^{\infty}\frac{1}{k+1}\frac{\Lambda_{\text{Tx}|R}^{k}}{k!}e^{-\Lambda_{\text{Tx}|R}}\\ &= \frac{1-e^{-\Lambda_{\text{Tx}|R}}}{\Lambda_{\text{Tx}|R}}.\end{aligned} \tag{24}$$

Using (23) and (24), we write the expected optimistic throughput-progress $\mathcal{T}^{\text{op}}$ as

$$\mathcal{T}^{\text{op}} = \mathbb{E}\left\{\frac{2R\,\eta\sin(\gamma/2)(1-e^{-\Lambda_{\text{Tx}|R}})}{\gamma\Lambda_{\text{Tx}|R}}\right\},$$

which can be calculated using (9) and (20) as

$$\begin{aligned}\mathcal{T}^{\text{op}} &= \frac{2\sin(\gamma/2)}{\pi\beta}\int_{0}^{r_c}\left(1-e^{-\lambda\pi\beta r^2}\right)e^{-\lambda\frac{\gamma}{2}r^2}\,\mathrm{d}r\\ &= \frac{\sqrt{2}\sin(\gamma/2)}{\sqrt{\lambda\gamma\pi}\beta}\Bigg[\operatorname{erf}\left(\sqrt{\log(\lambda/\epsilon)}\right)\\ &\qquad - \frac{\operatorname{erf}\left(\sqrt{\log(\lambda/\epsilon)(2\beta\frac{\pi}{\gamma}+1)}\right)}{\sqrt{2\beta\frac{\pi}{\gamma}+1}}\Bigg],\end{aligned} \tag{25}$$

where $\operatorname{erf}(x) = \frac{2}{\sqrt{\pi}}\int_0^x e^{-t^2}\,\mathrm{d}t$ denotes the error function. For $\frac{\epsilon}{\lambda} \ll 1$, we have that

$$\mathcal{T}^{\text{op}} \simeq \frac{\sqrt{2}\sin(\gamma/2)}{\sqrt{\lambda\gamma\pi}\beta}\left[1-\frac{1}{\sqrt{2\beta\frac{\pi}{\gamma}+1}}\right], \tag{26}$$

and we can conclude that

$$\mathcal{T}^{\text{op}} = \Theta\left(\frac{1}{\sqrt{\lambda}}\right). \tag{27}$$

In the case of $\mathcal{T}^{\text{pe}}$ we have to compute $\mathbb{E}^{\text{pe}}\{C|R\}$, according to

$$\begin{aligned}\mathbb{E}^{\text{pe}}\{C|R\} &= \mathbb{E}\left\{\frac{1}{I_{\text{Tx+Rx}}+1}\middle|R\right\}\\ &= \sum_{k=0}^{\infty}\frac{1}{k+1}\frac{\Lambda_{\text{Tx+Rx}|R}^{k}}{k!}e^{-\Lambda_{\text{Tx+Rx}|R}}\\ &= \frac{1-e^{-\Lambda_{\text{Tx+Rx}|R}}}{\Lambda_{\text{Tx+Rx}|R}}.\end{aligned} \tag{28}$$

Hence, $\mathcal{T}^{\text{pe}}$ can be written as

$$\mathcal{T}^{\text{pe}} = \mathbb{E}\left\{\frac{2R\sin(\gamma/2)(1-e^{-\Lambda_{\text{Tx+Rx}|R}})}{\gamma\Lambda_{\text{Tx+Rx}|R}}\right\}. \tag{29}$$

Using (17), (29) yields

$$\begin{aligned}\mathcal{T}^{\text{pe}} &= \frac{2\sin(\gamma/2)}{\pi\beta}\int_0^{r_c}\frac{1-e^{-\lambda\pi\beta(r^2+\frac{2}{\gamma\lambda})}}{r^2+\frac{2}{\gamma\lambda}}r^2e^{-\lambda\frac{\gamma}{2}r^2}\,\mathrm{d}r\\ &= \frac{2\sin(\gamma/2)}{\pi\beta}\Bigg[\int_0^{r_c}\frac{r^2e^{-\lambda\frac{\gamma}{2}r^2}}{r^2+\frac{2}{\gamma\lambda}}\,\mathrm{d}r\\ &\qquad - e^{-2\frac{\pi}{\gamma}\beta}\int_0^{r_c}\frac{r^2e^{-\lambda\frac{\gamma}{2}r^2(1+2\beta\frac{\pi}{\gamma})}}{r^2+\frac{2}{\gamma\lambda}}\,\mathrm{d}r\Bigg].\end{aligned} \tag{30}$$

For the case $\frac{\epsilon}{\lambda}\ll 1$, almost the complete probability mass of R is concentrated within the critical radius r_c. Thus, the error made by extending the upper integration border to infinity is negligible. With [17], the first integral in (30) then becomes

$$\begin{aligned}\int_0^{r_c}\frac{r^2e^{-\lambda\frac{\gamma}{2}r^2}}{r^2+\frac{2}{\gamma\lambda}}\,\mathrm{d}r &\simeq \int_0^{\infty}\frac{r^2e^{-\lambda\frac{\gamma}{2}r^2}}{r^2+\frac{2}{\gamma\lambda}}\,\mathrm{d}r\\ &= \sqrt{\frac{\pi}{2\lambda\gamma}}\left[1-e\sqrt{\pi}\left[1-\text{erf}(1)\right]\right]\\ &\simeq 0.243\sqrt{\frac{\pi}{2\lambda\gamma}}.\end{aligned} \tag{31}$$

Similarly, the second integral in (30) yields

$$\begin{aligned}\int_0^{r_c}\frac{r^2e^{-\lambda\frac{\gamma}{2}r^2(1+2\beta\frac{\pi}{\gamma})}}{r^2+\frac{2}{\gamma\lambda}}\mathrm{d}r &\simeq \int_0^{\infty}\frac{r^2e^{-\lambda\frac{\gamma}{2}r^2(1+2\beta\frac{\pi}{\gamma})}}{r^2+\frac{2}{\gamma\lambda}}\mathrm{d}r\\ &= \sqrt{\frac{\pi}{2\lambda\gamma}}\Bigg[\frac{1}{\sqrt{1+2\beta\frac{\pi}{\gamma}}}-\sqrt{\pi}e^{1+2\beta\frac{\pi}{\gamma}}\\ &\qquad\times\left[1-\text{erf}\left(\sqrt{1+2\beta\tfrac{\pi}{\gamma}}\right)\right]\Bigg].\end{aligned} \tag{32}$$

With (31) and (32), we can finally rewrite (30) as

$$\mathcal{T}^{\text{pe}} \simeq \frac{\sqrt{2}\sin(\gamma/2)}{\sqrt{\lambda\gamma\pi\beta}} \Bigg[0.243 - \frac{e^{-2\frac{\pi}{\gamma}\beta}}{\sqrt{1+2\beta\frac{\pi}{\gamma}}} + e\sqrt{\pi}\left[1 - \text{erf}\left(\sqrt{1+2\beta\tfrac{\pi}{\gamma}}\right)\right] \Bigg]$$
$$= \Theta\left(\frac{1}{\sqrt{\lambda}}\right). \tag{33}$$

Since $\mathcal{T}^{\text{pe}} \leq \mathcal{T} \leq \mathcal{T}^{\text{op}}$, it follows that $\mathcal{T} = \Theta\left(\frac{1}{\sqrt{\lambda}}\right)$. This proves the first part of Theorem 1.

B. Expected Packet Delay normalized to the one-hop Progress

Similarly as in the case of $\mathcal{T}$, we decompose (2) according to the law of total expectation. Assuming $\alpha = 1$, $\mathcal{D}$ can be written as

$$\mathcal{D} = \mathbb{E}\left\{\mathbb{E}\left\{Z^{-1}|R\right\}\right\}, \tag{34}$$

where the inner expectation can be computed using (10) as

$$\mathbb{E}\left\{Z^{-1}|R\right\} = \frac{2}{R\gamma}\log\frac{1+\sin(\gamma/2)}{\cos(\gamma/2)}. \tag{35}$$

With (35) we can calculate $\mathcal{D}$ as

$$\mathcal{D} = \mathbb{E}\left\{\frac{2}{R\gamma}\log\frac{1+\sin(\gamma/2)}{\cos(\gamma/2)}\right\}$$
$$= 2\lambda\log\frac{1+\sin(\gamma/2)}{\cos(\gamma/2)}\int_0^{r_c} e^{-\lambda\frac{\gamma}{2}r^2}\,\mathrm{d}r$$
$$= \sqrt{\frac{2\lambda\pi}{\gamma}}\log\frac{1+\sin(\gamma/2)}{\cos(\gamma/2)}\,\text{erf}\left(\sqrt{\log(\lambda/\epsilon)}\right)$$
$$= \Theta\left(\sqrt{\lambda}\right). \tag{36}$$

This proves the second part of Theorem 1. Note that $\mathcal{D}$ has a singularity at $\gamma = \pi$ which implies that the first moment of the delay exists only for $\gamma < \pi$.

V. Implications

The outcome of this analysis suggests that the expected per-node throughput in random networks approaches the upper bound in the scaling sense if nodes employ power control in conjunction with a nearest neighbor forwarding strategy. In this case, the expected delay for a randomly chosen transmitter-receiver pair approaches the lower bound in the scaling sense. Note that these results are obtained while ensuring connectivity (with probability $1-\epsilon$, where $0 < \epsilon \ll 1$) in the network. Hence, we state that the throughput-connectivity trade-off can be resolved: by ensuring

connectivity we can use a simple routing scheme and due to power control, we do not have to drive the network in the self-interference limited regime.

The gain of the NFP strategy can be best illustrated by comparing it to its counterpart, namely the MVR strategy. Recall that while NFP minimizes spatial contention, MVR intends to maximize the progress Z and thus increases spatial contention. If we consider now the case $\frac{\epsilon}{\lambda} \to 0$ we find that in the MVR strategy $Z \simeq R \simeq r_c$, since a node can follow this strategy better and better due to the fact that the average number of potential relays increases with $\log \lambda$. In this case, power control has no effect anymore and the network model becomes similar to the one in [1]. Hence, we expect that employing the MVR strategy results in an expected per-node throughput of $\mathcal{T} = \Theta\left(\frac{1}{\sqrt{\lambda \log \lambda}}\right)$. From [6] we can obtain the PDF of Z and the conditional PDF of R given Z, so that we can first decompose and then calculate $\mathcal{T}$ and $\mathcal{D}$ in a similar fashion as in the case of NFP. Fig. 3 shows the scaling behavior of the expected throughput-progress $\mathcal{T}$ for the two forwarding strategies. The results for the MVR strategy were obtained through numerical integration techniques. From Fig. 3 it can be seen that $\mathcal{T}$ is consistent with the results in [1] for the MVR strategy.

Fig. 4 shows the scaling behavior of the expected packet delay normalized to the one-hop progress $\mathcal{D}$ for the two forwarding strategies. In the case of NFP, the central angle was set to $\gamma = 0.9\,\pi$. Note that $\mathcal{D}$ has a singularity at $\gamma = \pi$ since $\mathbb{E}\left\{\frac{1}{Z}\middle| R\right\}$ does not exist in this case. Again, the results for the MVR strategy are consistent with prior literature [18]. In the case of NFP, $\mathcal{T}$ and $\mathcal{D}$ achieve the optimal throughput-delay trade-off introduced in [18] for a fixed wireless network.

Due to the independence between the hops, we can obtain the expected per-node throughput by dividing $\mathcal{T}$ by the expected path length on a sphere with unit area, which is $\frac{\pi}{2}$, as well as the expected delay by multiplying $\mathcal{D}$ by $\frac{\pi}{2}$. Furthermore, the results can be scaled by $\sqrt{A}$ for arbitrary large spheres.

An interesting fact of the NFP strategy is the scaling behavior of the expected split of resources a typical node experiences, i.e., the limits $\lim_{\lambda\to\infty} \mathbb{E}\{I+1\}$ and $\lim_{\lambda\to\infty} \mathbb{E}\{\frac{1}{I+1}\}$. These values can be bounded by

$$1 + 2\beta\frac{\pi}{\gamma} \leq \lim_{\lambda\to\infty} \mathbb{E}\{I+1\} \leq 1 + 4\beta\frac{\pi}{\gamma} \tag{37}$$

and

$$\begin{aligned} &\frac{e\gamma}{2\beta\pi}\left[\mathrm{Ei}_1(1) - \mathrm{Ei}_1\left(1 + 2\beta\tfrac{\pi}{\gamma}\right)\right] \\ &\qquad \leq \lim_{\lambda\to\infty} \mathbb{E}\left\{\frac{1}{I+1}\right\} \leq \frac{\gamma}{2\beta\pi}\log\left[1 + 2\beta\tfrac{\pi}{\gamma}\right], \end{aligned} \tag{38}$$

respectively, where $\mathrm{Ei}_1(z) = \int_1^\infty t^{-1}e^{zt}\,\mathrm{d}t$ is the exponential integral. It can be seen from (37) and (38) that the expected split of resources, either representing the delay or the throughput, converges toward a constant which is independent from λ. This constant depends only on the traffic intensity β and on the central angle γ. Hence, the amount of spatial contention is independent of the network size for the NFP strategy.

Fig. 5 shows the impact of the traffic intensity β on the expected per-node throughput $\mathcal{T}$ for a fixed λ. It can be seen that for large β, i.e., high network load and/or large guard zone, the NFP performs better than the MVR strategy. This is because self-interference is the limiting performance factor in the high traffic regime. However, for

low β, spatial contention is comparably small and performance is mainly determined by the one-hop progress Z, i.e., $\mathcal{T} \simeq \mathbb{E}\{Z\}$ and $\mathcal{D} \simeq \mathbb{E}\left\{\frac{1}{Z}\right\}$. In this low traffic regime, MVR becomes superior since Z is maximized with this strategy. An optimal forwarding scheme should therefore use an adaptive strategy, taking into account the actual traffic intensity β in order to maximize throughput or minimize delay, respectively.

VI. Conclusion

We addressed the question if the throughput-connectivity trade-off in random networks can be resolved when nodes are allowed to employ power control. The idea behind this is that nodes can set their transmission ranges such that connectivity in the network is ensured (with probability $1-\epsilon$, where $0<\epsilon\ll 1$) while they can reduce their actual transmission power within this range (in order to minimize spatial contention). In this work, power control simply had to compensate for the path loss to ensure a certain received signal strength at the receivers. Furthermore, greedy geographic forwarding was used for modeling the routing scheme. It was found that if nodes use power control in conjunction with a simple nearest neighbor forwarding strategy, i.e., nodes transmit only to their nearest neighbor, the expected per-node throughput is $\Theta\left(\frac{1}{\sqrt{\lambda}}\right)$, while connectivity is ensured with probability $1-\epsilon$. Similarly, the expected delay was found to be $\Theta\left(\sqrt{\lambda}\right)$.

Furthermore, we compared the nearest neighbor forwarding strategy NFP to its counterpart strategy MVR, which intends to maximize the one-hop progress. It was found that the latter strategy outperforms the former one in terms of both expected per-node throughput and delay for low traffic intensities, i.e., small network loads and small spectral efficiencies. This is because in the low traffic regime, performance is mainly determined by the amount of one-hop progress rather than spatial contention. For high traffic intensities, we found that the NFP strategy performs better because it minimizes spatial contention. We also showed through numerical computation that the expected per-node throughput and the expected delay are $\Theta\left(\frac{1}{\sqrt{\lambda}\log\lambda}\right)$ and $\Theta\left(\sqrt{\frac{\lambda}{\log\lambda}}\right)$ for the MVR strategy which is consistent with the results obtained for random networks in [1].

We conclude that the throughput-connectivity trade-off in random networks can generally be resolved if we take into account power control as an additionally degree of freedom. If nodes in a random network employ power control in such a way that they can follow a simple nearest neighbor forwarding strategy, the expected per-node throughput scales with the upper bound $\Theta\left(\frac{1}{\sqrt{\lambda}}\right)$. In this case, throughput and delay achieve the optimal throughput-delay scaling trade-off.

VII. Critical radius for global connectivity

Let the random variable ζ_i denote the degree of node X_i in the forwarding area, i.e., the number of neighbors of node X_i in a circle sector with central angle γ and radius r_c (see Fig. 1). The ζ_i are Poisson distributed with intensity $\lambda\frac{\gamma}{2}r_c^2$. Then, global connectivity is defined as the joint event of all nodes X_i finding at least one node ($\zeta_i \geq 1$) in the forwarding area. To determine r_c, we let the probability of the complimentary event to be at most

ϵ, $0<\epsilon\ll 1$, i.e.,

$$\begin{aligned}\epsilon &\geq \mathbb{P}\{\zeta_1=0\}+\mathbb{P}\{\zeta_2=0\}\mathbb{P}\{\zeta_1\geq 1\}+\cdots\\ &\quad+\mathbb{P}\{\zeta_\lambda=0\}\mathbb{P}\{\zeta_1\geq 1,\ldots,\zeta_{\lambda-1}\geq 1\}\\ &=\sum_{k=1}^{\lambda}\mathbb{P}\{\zeta_k=0\}\mathbb{P}\left\{\bigcap_{\ell=1}^{k-1}\zeta_\ell\geq 1\right\}. \end{aligned} \tag{39}$$

Neglecting the second probability in the sum, we find that

$$\sum_{k=1}^{\lambda}\mathbb{P}\{\zeta_k=0\}=\lambda e^{-\lambda\frac{\gamma}{2}r^2}\leq\epsilon \tag{40}$$

is a sufficient condition for the complementary event. Solving $\lambda e^{-\lambda\frac{\gamma}{2}r^2}\leq\epsilon$ in (40) for r yields the critical radius

$$r_c=\sqrt{2\frac{\log\lambda-\log\epsilon}{\lambda\gamma}}. \tag{41}$$

Note that by substituting $c:=\log\frac{1}{\epsilon}$ with $\lim_{\lambda\to\infty}\epsilon(\lambda)=0$, we obtain a similar result for asymptotic connectivity as in [3].

REFERENCES

[1] P. Gupta and P. R. Kumar, "The capacity of wireless networks," *Information Theory, IEEE Transactions on*, vol. 46, no. 2, pp. 388–404, 2000.

[2] S. R. Kulkarni and P. Viswanath, "A deterministic approach to throughput scaling in wireless networks," *IEEE Trans. on Information Theory*, vol. 50, pp. 1041–1049, 2004.

[3] P. Gupta and P. Kumar, "Critical power for asymptotic connectivity," in *Decision and Control, 1998. Proceedings of the 37th IEEE Conference on*, vol. 1, 1998, pp. 1106–1110 vol.1.

[4] M. Franceschetti, O. Dousse, D. N. C. Tse, and P. Thiran, "Closing the gap in the capacity of wireless networks via percolation theory," *IEEE Trans. Information Theory*, vol. 53, pp. 1009–1018, 2007.

[5] F. Xue and P. R. Kumar, *Scaling Laws for Ad Hoc Wireless Networks: An Information Theoretic Approach*, ser. Foundations and Trends in Networking. Now Publishers, vol. 1, no. 2.

[6] T.-C. Hou and V. Li, "Transmission range control in multihop packet radio networks," *Communications, IEEE Transactions on*, vol. 34, no. 1, pp. 38–44, Jan 1986.

[7] I. Stojmenovic, "Position-based routing in ad hoc networks," 2002.

[8] A. Jovicic, S. Kulkarni, and P. Viswanath, "Upper bounds to transport capacity of wireless networks," in *Decision and Control, 2003. Proceedings. 42nd IEEE Conference on*, vol. 3, 9-12 2003, pp. 3136 – 3141 Vol.3.

[9] J. Li, C. Blake, D. S. J. De Couto, H. I. Lee, and R. Morris, "Capacity of ad hoc wireless networks," in *Proceedings of the 7th ACM International Conference on Mobile Computing and Networking*, Rome, Italy, July 2001, pp. 61–69.

[10] S. Weber, J. G. Andrews, and N. Jindal, "A tutorial on transmission capacity," 2008. [Online]. Available: http://www.citebase.org/abstract?id=oai:arXiv.org:0809.0016

[11] M. Haenggi, "Outage and local throughput and capacity of random wireless networks," 2008. [Online]. Available: http://www.citebase.org/abstract?id=oai:arXiv.org:0806.0909

[12] O. Dousse and P. Thiran, "Connectivity vs capacity in dense ad hoc networks," in *INFOCOM 2004. Twenty-third AnnualJoint Conference of the IEEE Computer and Communications Societies*, vol. 1, 7-11 2004, p. 486.

[13] O. Dousse, M. Franceschetti, and P. Thiran, "On the throughput scaling of wireless relay networks," *Information Theory, IEEE Transactions on*, vol. 52, no. 6, pp. 2756 –2761, june 2006.

[14] M. Haenggi, J. Andrews, F. Baccelli, O. Dousse, and M. Franceschetti, "Stochastic geometry and random graphs for the analysis and design of wireless networks," *Selected Areas in Communications, IEEE Journal on*, vol. 27, no. 7, pp. 1029–1046, September 2009.

[15] M. Mauve, J. Widmer, and H. Hartenstein, "A survey on position-based routing in mobile ad-hoc networks," *IEEE Network*, vol. 15, pp. 30–39, 2001.

[16] M. Haenggi, "On distances in uniformly random networks," *Information Theory, IEEE Transactions on*, vol. 51, no. 10, pp. 3584 –3586, oct. 2005.

[17] I.S.Gradshteyn and I.M.Ryzhik, *Table of Integrals, Series, and Products*, 6th ed., A. Jeffrey and D. Zwillinger, Eds. Academic Press, 2000.

[18] A. E. Gamal, J. Mammen, B. Prabhakar, and D. Shah, "Throughput-delay trade-off in wireless networks," in *In Proc. of IEEE Infocom*, 2004.

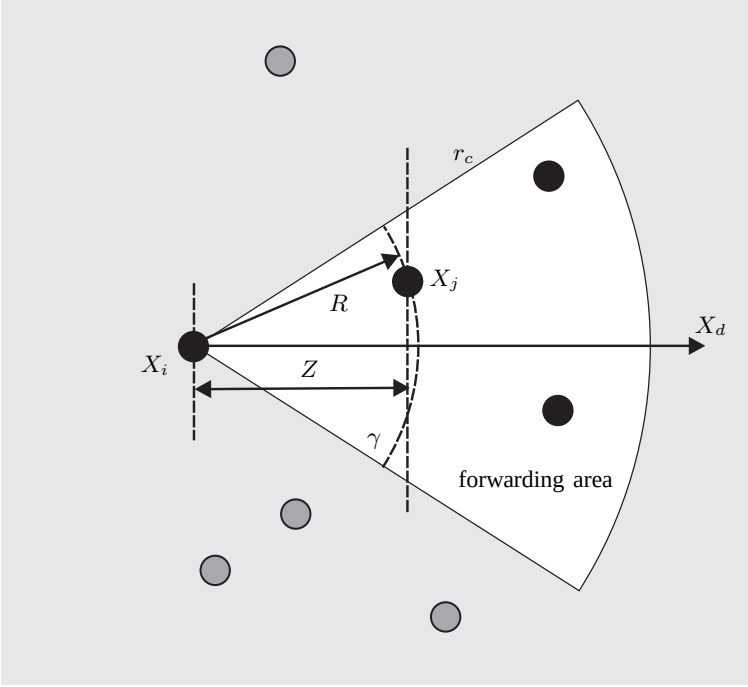

Fig. 1. The NFP scheme: only nodes that are within the forwarding area (white area) are considered as potential relays. Node X_i currently holding the packet selects node X_j as relay since this node realizes (7).

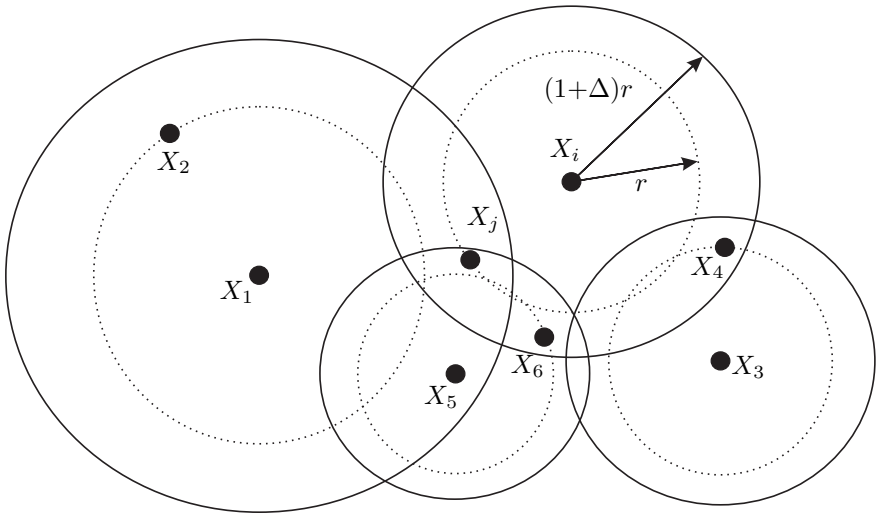

Fig. 2. Illustration of the problem of counting violations twice: the number of violations regarding the reference receiver X_j is 2 (pairs $\{X_1, X_2\}$ and $\{X_5, X_6\}$). Number of violations regarding the reference transmitter X_i is 2 (pairs $\{X_3, X_4\}$ and $\{X_5, X_6\}$). Hence, the violation created by the pair $\{X_5, X_6\}$ is considered twice.

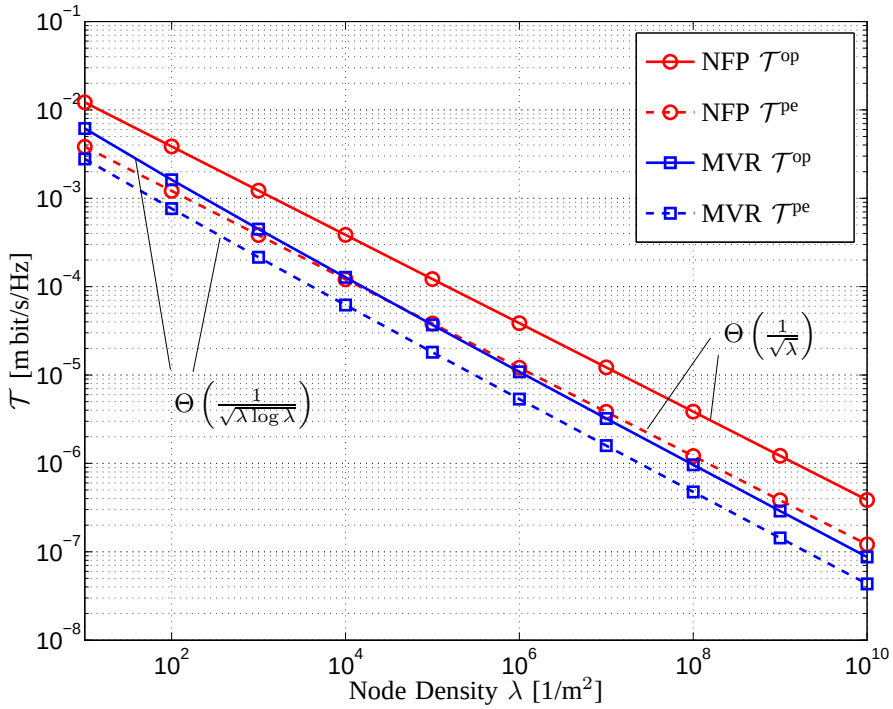

Fig. 3. Expected Throughput-Progress $\mathcal{T}$ for MVR and NFP. Guard zone $\Delta = 1$, network load $p = 1$, central angle $\gamma = \pi$, spectral efficiency $\eta = 1$ and connectivity is ensured with probability $1 - \epsilon = 0.99$.

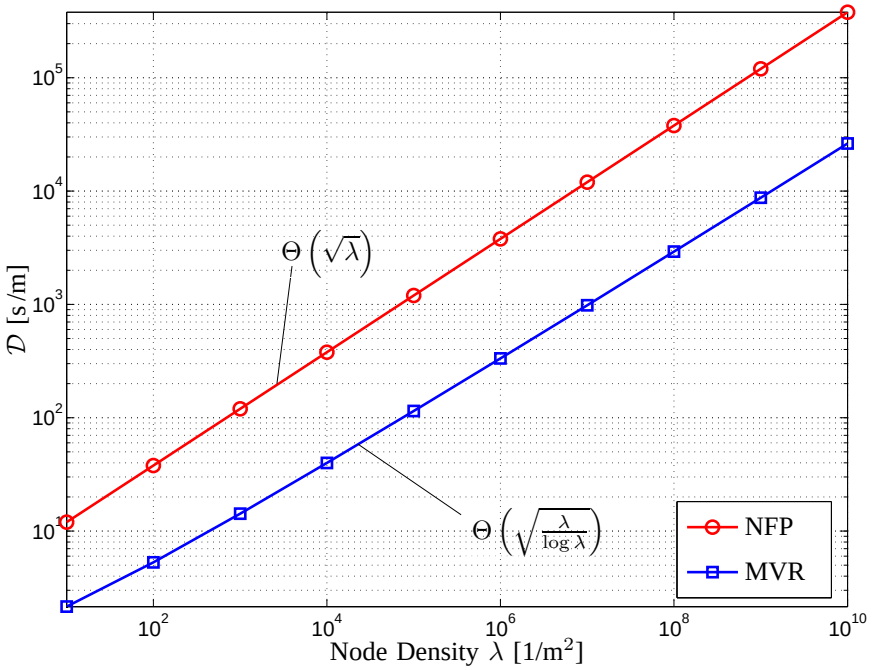

Fig. 4. Expected packet delay normalized to the one-hop progress $\mathcal{D}$ for MVR and NFP. Guard zone $\Delta = 1$, network load $p = 1$, central angle $\gamma = 0.9\,\pi$, constant one-hop delay $\alpha = 1$ and connectivity is ensured with probability $1 - \epsilon = 0.99$.

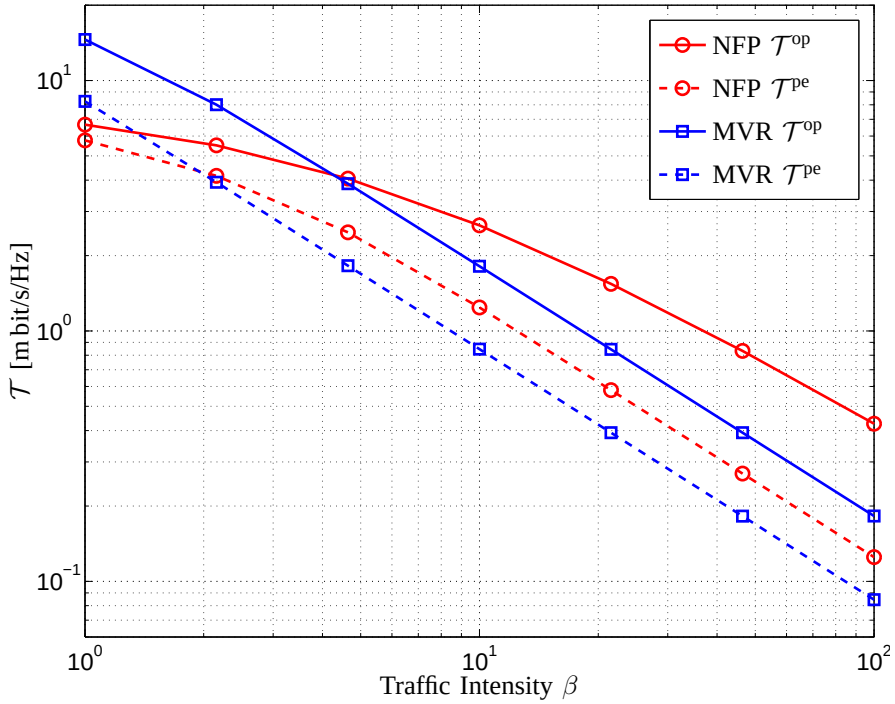

Fig. 5. Expected throughput-progress $\mathcal{T}$ vs. traffic intensity β for $\lambda = 30$ nodes. The area is set to $|A| = 10^4$ m^2 and connectivity is ensured with probability $1 - \epsilon = 0.99$.